

Note

Heat Conservation in Deforming Element Phase Change Simulation

INTRODUCTION

In a series of previous papers [8-10, 6], a technique for finite element phase change simulation has been developed and tested. The essential feature of this technique is the use of the Galerkin method on deforming elements, with the element motion tied to the phase boundary and interpolated at interior nodes. In this paper, we demonstrate that this method conserves heat exactly, provided the calculation of the heat flux at the phase boundary is reformulated.

The new boundary condition requires no restructuring of the basic algorithm and adds no computational overhead. Further, it eliminates a small but persistent error, which we have observed and reported in the earlier papers: a consistent overprediction of the phase boundary penetration (roughly 1-3%) for freezing problems. The present heat balance analysis reveals that this has been a first-order error in the mesh spacing normal to the phase boundary, which explains its persistence even when the temperature solution was well resolved.

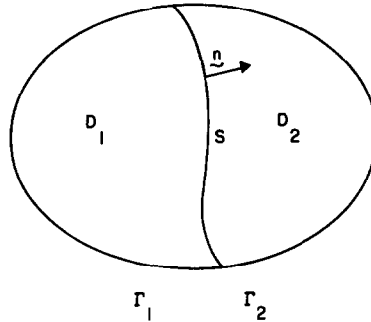
Computational results confirm that the new boundary condition yields second-order accuracy overall and errors which are an order of magnitude smaller than those previously reported.

PROBLEM STATEMENT AND METHOD

Consider a domain D occupied by two phases, separated by an interface S as in Fig. 1. By convention, the normal vector on S is directed from D_1 into D_2 . The Stefan problem consists of the heat equation on D_1 and D_2 separately. In Galerkin form, we have

$$\left\langle c \frac{\partial \hat{T}}{\partial t}, \phi_i \right\rangle + \langle K \nabla \hat{T}, \nabla \phi_i \rangle = F_i, \quad (1)$$

where $\langle \rangle$ is the inner product notation representing the sum of integrations over each phase, ϕ_i are the finite element bases, and \hat{T} is the approximate numerical solution. The quantity F_i arises from the integration of the divergence term by parts

FIG. 1. Two-phase domain with interface S .

and has two components corresponding to the flux integrals over Γ and S , respectively,

$$F_i = F_i^\Gamma + F_i^S = \oint_{\Gamma} K \nabla T \cdot \mathbf{n} \phi_i \, ds + \int_S \{ (K \nabla T)_1 - (K \nabla T)_2 \} \cdot \mathbf{n} \phi_i \, ds. \quad (2)$$

The usual boundary conditions apply on Γ , and two interface conditions are required on S ,

$$T = T_0, \quad (3)$$

$$L \mathbf{V} \cdot \mathbf{n} = \{ (K \nabla T)_1 - (K \nabla T)_2 \} \cdot \mathbf{n}, \quad (4)$$

where \mathbf{V} is the motion of S and T_0 is the phase change temperature.

In all of the previous papers in this series, the phase boundary has been treated as a type I (Dirichlet) boundary: Equation (3) was satisfied exactly, and the associated Galerkin equations eliminated, following conventional practice for the heat equation. The practical effect has been that all inner products in (1) are evaluated over a single phase only, and the quantities F_i^S never appear in the formulation. Satisfaction of the moving boundary condition (4) thus required differentiation of \hat{T} , a feature also elaborated by others [1-3]. The multidimensional technique suggested by Lynch [6] is

$$L \mathbf{V}_i \cdot \int_S \hat{\mathbf{n}} \phi_i \, ds = \hat{F}_i^S \equiv \int_S \{ (K \nabla \hat{T})_1 - (K \nabla \hat{T})_2 \} \cdot \hat{\mathbf{n}} \phi_i \, ds, \quad (5)$$

where \mathbf{V}_i is the velocity of node i , and \hat{F}_i^S differs from F_i^S insofar as the actual computed temperature gradient appears. The obvious connection between these boundary fluxes suggests the alternative

$$L \mathbf{V}_i \cdot \int_S \hat{\mathbf{n}} \phi_i \, ds = F_i^S, \quad (6)$$

which, when substituted into the Galerkin equation (1), yields

$$\left\langle c \frac{\partial \hat{T}}{\partial t}, \phi_i \right\rangle + \langle K \nabla \hat{T}, \nabla \phi_i \rangle = F_i^r + L \mathbf{V}_i \cdot \int_S \hat{\mathbf{n}} \phi_i ds. \tag{7}$$

The previously discarded Galerkin equation on S is seen, in the form (7), to be “the equation for $\hat{\mathbf{V}} \cdot \mathbf{n}$.”

In the same spirit we may substitute the boundary condition (4) directly into F_i^s in (1), which yields the alternative

$$\left\langle c \frac{\partial \hat{T}}{\partial t}, \phi_i \right\rangle + \langle K \nabla \hat{T}, \nabla \phi_i \rangle = F_i^r + \int_S L \hat{\mathbf{V}} \cdot \hat{\mathbf{n}} \phi_i ds = F_i^r + L \sum_j \mathbf{V}_j \cdot \int_S \hat{\mathbf{n}} \phi_j \phi_i ds. \tag{8}$$

In one dimension, (7) and (8) are the same. In higher dimensions, the expression for F_i^s in (7) is effectively a lumped representation of that in (8). Below it is shown that calculation of the phase boundary motion according to either (7) or (8) leads to a perfect heat balance; while the conventional practice produces a numerical heat imbalance which is first order in the mesh spacing normal to S .

CONSERVATION RELATIONS

The statement of thermal energy conservation for the system of Fig 1 may be obtained by integrating the heat equation over both phases, and applying the divergence theorem

$$\left\langle c \frac{\partial T}{\partial t} \right\rangle = \oint_R K \nabla T \cdot \mathbf{n} ds + \int_S \{ (K \nabla T)_1 - (K \nabla T)_2 \} \cdot \mathbf{n} ds \tag{9}$$

or, in light of the boundary condition (2),

$$\left\langle c \frac{\partial T}{\partial t} \right\rangle = \oint_R K \nabla T \cdot \mathbf{n} ds + \int_S L \mathbf{V} \cdot \mathbf{n} ds. \tag{10}$$

On the assumption that $c = c(T, \mathbf{x})$, we introduce $H(T, \mathbf{x}) = \int_{T_0}^T c(\theta, \mathbf{x}) d\theta$. (Note that $H = 0$ on S ; latent heat is excluded from H by convention here.) With all system boundaries in motion with velocity \mathbf{V} , the left side of (10) becomes

$$\left\langle c \frac{\partial T}{\partial t} \right\rangle = \left\langle \frac{\partial H}{\partial t} \right\rangle = \frac{d}{dt} \langle H \rangle - \oint_R H \mathbf{V} \cdot \mathbf{n} ds \tag{11}$$

and therefore

$$\frac{d}{dt} \langle H \rangle = \oint_R (H \mathbf{V} + K \nabla T) \cdot \mathbf{n} ds + \int_S L \mathbf{V} \cdot \mathbf{n} ds. \tag{12}$$

If \mathcal{V}_2 is the volume occupied by phase 2,

$$\frac{d}{dt} \{ \langle H \rangle + L\mathcal{V}_2 \} = \oint_{\Gamma} (HV + K\nabla T) \cdot \mathbf{n} \, ds + \int_{\Gamma_2} L\mathbf{V} \cdot \mathbf{n} \, ds \quad (13)$$

where $\{ \langle H \rangle + L\mathcal{V}_2 \}$ is the heat content of the system.

The numerical heat balance is derived by summing the Galerkin equations actually solved. The inner products $\langle \rangle$ are typically approximated by numerical quadrature, which we indicate by $[]$. Assuming that none of the Galerkin equations are discarded, we have $\sum \phi_i = 1$ and $\sum \nabla \phi_i = 0$ everywhere. Thus, summation of either (7) or (8), with $[]$ substituted for $\langle \rangle$, produces the same result,

$$\left[c \frac{\partial \hat{T}}{\partial t} \right] = \oint_{\Gamma} K\nabla T \cdot \mathbf{n} \, ds + \int_S L\hat{\mathbf{V}} \cdot \hat{\mathbf{n}} \, ds, \quad (14)$$

where the integral over Γ , representing the conduction flux, is the sum of the F_i^T . If the quadrature is sufficient to exactly integrate $\langle c \partial \hat{T} / \partial t \rangle$, then all of the steps leading to (13) from (10) can be retraced. More generally, we introduce the quadrature error \mathcal{E}_q ,

$$\mathcal{E}_q = \left\langle c \frac{\partial \hat{T}}{\partial t} \right\rangle - \left[c \frac{\partial \hat{T}}{\partial t} \right] \quad (15)$$

and (14) leads to a result exactly analogous to (13),

$$\frac{d}{dt} \{ \langle \hat{H} \rangle + L\hat{\mathcal{V}}_2 \} = \oint_{\Gamma} \hat{H}\hat{\mathbf{V}} \cdot \hat{\mathbf{n}} \, ds + \oint_{\Gamma} K\nabla T \cdot \mathbf{n} \, ds + \int_{\Gamma_2} L\hat{\mathbf{V}} \cdot \hat{\mathbf{n}} \, ds + \mathcal{E}_q. \quad (16)$$

Thus, provided the quadrature is sufficient to make \mathcal{E}_q vanish, the formulations (7) and (8) exactly conserve heat. The key ingredient in these formulations is the use of the Galerkin equations along the phase boundary for the heat flux F_i^S . Conventional flux calculations based on $\nabla \hat{T}$ only provide an approximate value \hat{F}_i^S , the impact of which is quantified below.

CARTESIAN ANALYSIS AND TESTS

Consider a one-phase, one-dimensional Stefan problem on N equal-length linear elements, with node $\#0$ fixed at the origin and node $\#N$ tracking the phase boundary, $X_N = S(t)$. Constant coefficients are assumed. The conventional calculation of the phase front velocity, indicated by the superscript c , is

$$LV_N^c = \hat{F}_N = K \left. \frac{\partial \hat{T}}{\partial x} \right|_N \quad (17)$$

while the Galerkin formulation (7) or (8) yields

$$LV_N^G = F_N = \left\langle c \frac{\partial \hat{T}}{\partial t}, \phi_N \right\rangle + \left\langle K \frac{\partial \hat{T}}{\partial x}, \frac{\partial \phi_N}{\partial x} \right\rangle. \quad (18)$$

Direct calculation of the last term in (18) yields exactly \hat{F}_N in this special case, and thus

$$LV_N^G = \left\langle c \frac{\partial \hat{T}}{\partial t}, \phi_N \right\rangle + K \left. \frac{\partial \hat{T}}{\partial x} \right|_N \quad (19)$$

Evidently the Galerkin calculation contains a correction in the form of a heat storage term. For simple freezing problems this correction is negative and thus V_N^c errs on the high side. This is precisely the consistent trend observed previously (Lynch and O'Neill, 1981). Note that due to the integral form of the correction, it will be linear in Δx .

To analyze the accumulated error in $S(t)$, Eqs. (17) and (19) may be further simplified and integrated exactly for typical Neumann problems. A characteristic of these simple simulations is that nodal temperatures stabilize very quickly and a self-similar numerical solution is produced: $\hat{T}(x, t) \rightarrow \hat{T}(\chi)$, where $\chi = x/S(t)$. Further, $\hat{T}(\chi)$ is quite insensitive to the treatment of the phase boundary condition, the primary numerical distinction being in the location of $S(t)$. Thus, $\partial \hat{T}/\partial x|_N \simeq (d\hat{T}/d\chi|_N)/S(t)$, and (17) may be integrated to yield

$$\left(\frac{S^2}{2} \right)^c = 2t \left. \frac{K d\hat{T}}{L d\chi} \right|_N. \quad (20)$$

For the Galerkin treatment (19), we have $dT_i/dt \simeq 0$ and thus $\partial \hat{T}/\partial t \simeq -V \partial \hat{T}/\partial x$,

$$LV_N^G = -c \left. \frac{\partial \hat{T}}{\partial x} \right|_N (V_{N-1} + 2V_N) \frac{\Delta x}{6} + K \left. \frac{\partial \hat{T}}{\partial x} \right|_N. \quad (21)$$

For this simple grid $\Delta x = S/N$ and $V_i = (i/N)(dS/dt)$, and (21) becomes

$$L \frac{dS}{dt} = K \left. \frac{\partial \hat{T}}{\partial x} \right|_N \left[1 - \frac{c}{K} \frac{S}{2N} \left(1 - \frac{1}{3N} \right) \frac{dS}{dt} \right] \quad (22)$$

which, with the above assumption concerning $\partial \hat{T}/\partial x$, may be integrated to give

$$S^G = S^c / \left[1 + \frac{c}{L} \left. \frac{d\hat{T}}{d\chi} \right|_N \frac{1}{2N} \left(1 - \frac{1}{3N} \right) \right]^{1/2}. \quad (23)$$

An estimate for $d\hat{T}/d\chi|_N$ is its analytic value¹ $2\lambda^2 L/c$, and (23) becomes

$$\frac{S^G}{S^c} = \left[1 + \frac{\lambda^2}{N} \left(1 - \frac{1}{3N} \right) \right]^{1/2} \simeq \left[1 + \frac{\lambda^2}{2N} \right]. \quad (24)$$

¹ Analytically, $S = \lambda \sqrt{4(K/c)t}$.

Thus an estimate for the relative overprediction of S by S^c is $\lambda^2/2N$. For small Stefan numbers, $\lambda^2 \approx S_i/2$, where $S_i = c\Delta T/L$, and a simpler error estimate is $S_i/4N$.

To confirm this analysis numerically, a mesh of N linear elements was initialized with thermal properties as in [10], and the solution was advanced by M time steps such that the frozen thickness would grow by a factor of 10. The error in \hat{S} relative to the analytic value is reported at the end of the simulation: $E = \hat{S}/S - 1$. In Fig. 2 we show the results obtained with the conventional flux calculation versus N at three levels of refinement in the time domain. The temporal discretization error is effectively suppressed relative to the spatial error at $M = 64$, and it is evident that the error decreases only linearly with N , as predicted above. In Fig. 3 we isolate the temporal discretization error by subtracting the spatial part, i.e., the error obtained with $M = 64$ and the same value of N . Evidently the temporal discretization error is second order, as expected, and is quite small relative to the spatial error.

Experiments with the Galerkin flux calculation also show a small second-order temporal error. Significantly, however, the spatial error is second-order as illustrated in Fig. 4 for $M = 64$. In the range of parameters reported, the overall error was reduced by about an order of magnitude relative to the conventional

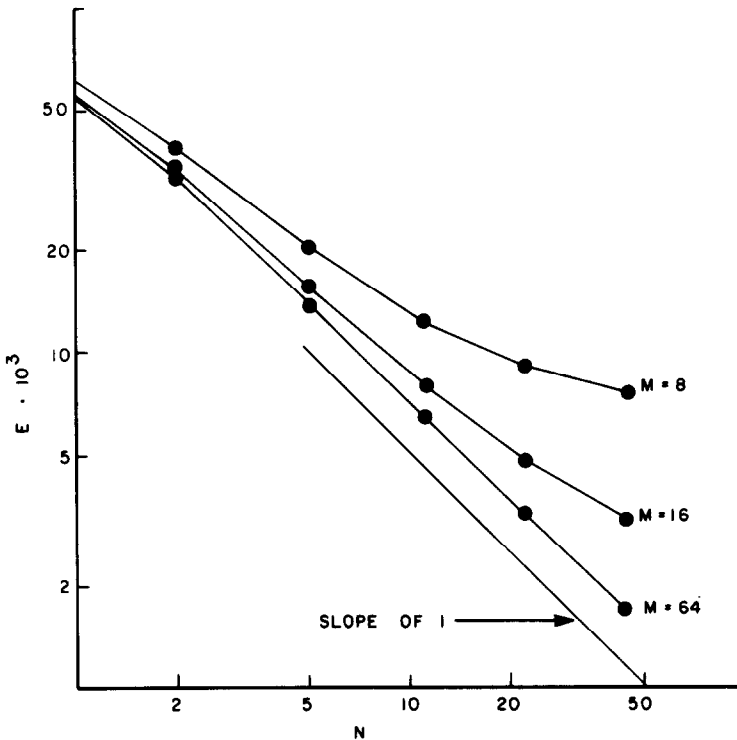


FIG. 2. Total relative error E using the conventional flux calculation versus number of elements N for 1-D, 1-phase Cartesian tests.

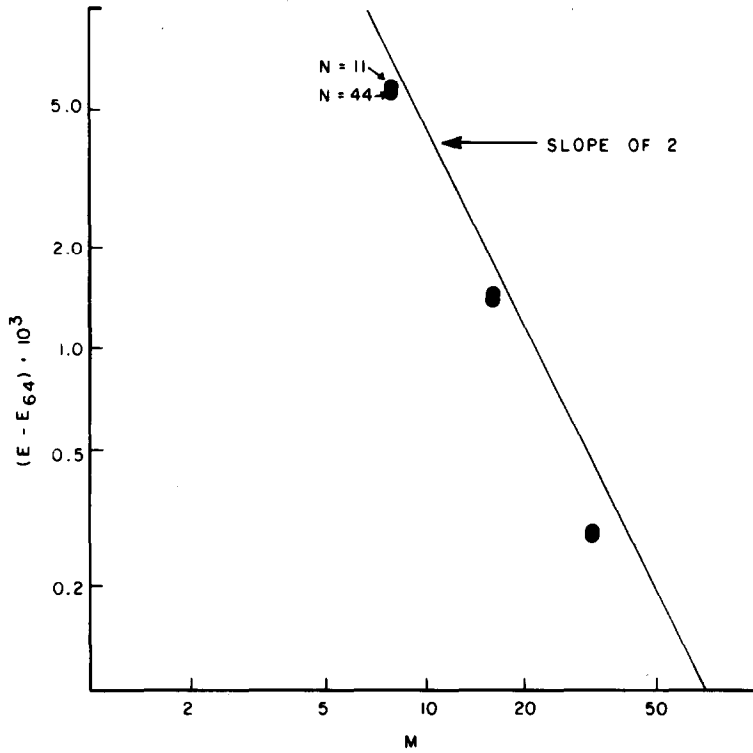


FIG. 3. Isolated temporal error using conventional flux calculation versus time steps M for 1-D, 1-phase Cartesian tests.

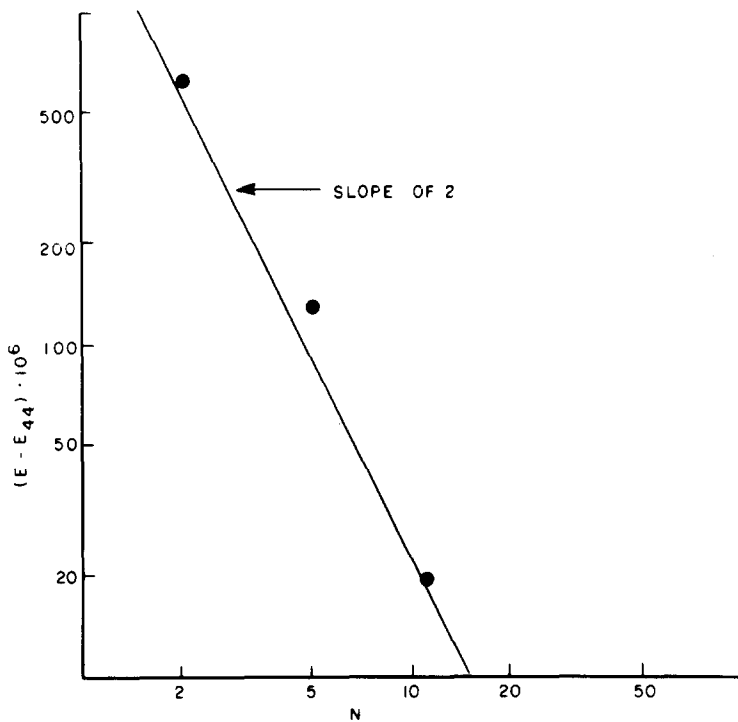


FIG. 4. Isolated spatial error using Galerkin flux calculation versus number of elements N for 1-D, 1-phase Cartesian tests.

TABLE I
One-phase Neumann Problem^a

N	E^G	E^c	$\lambda^2/2N$
44	0.119×10^{-3}	1.72×10^{-3}	1.79×10^{-3}
22	0.115×10^{-3}	3.31×10^{-3}	3.58×10^{-3}
11	0.0992×10^{-3}	6.46×10^{-3}	7.17×10^{-3}
5	-0.0157×10^{-3}	13.8×10^{-3}	15.8×10^{-3}
2	-0.517×10^{-3}	32.3×10^{-3}	39.4×10^{-3}

^a Computed error, $E = \hat{S}/S - 1$, versus number of elements (N) for conventional (c) and Galerkin (G) flux calculations; $\lambda^2/2N$ is the error estimate; the temporal resolution is high, $M = 64$.

results. Thus in Fig. 4 we have isolated the spatial error by subtracting the temporal error—i.e., the error obtained with $N = 44$ and the same value of M .

In Table I we list the total computed error versus N for the conventional and Galerkin flux calculations. The estimate $\lambda^2/2N$ is evidently quite good for reasonable values of N .

In the two-phase version of this problem the same trends emerge: consistent over-prediction of S by the conventional flux calculation, with first-order error in the mesh spacing and second-order in the time step; and smaller errors which are second-order in N and M when the Galerkin procedure is used. As in the one-phase case, the Galerkin expression for the heat flux differs from the conventional by the term $\langle c(\partial \hat{T}/\partial t), \phi_N \rangle$, but now the inner product extends over both phases. The conventional error is thus larger, and proportional to the element size on both sides of S . Some typical results are displayed in Table II. The Galerkin errors are generally an order of magnitude smaller than the conventional errors.

TABLE II
Two-phase Neumann Problem^a

N	E^G	E^c
44	0.0840×10^{-3}	2.74×10^{-3}
22	0.0740×10^{-3}	5.40×10^{-3}
11	0.0325×10^{-3}	10.8×10^{-3}
5	-0.184×10^{-3}	23.8×10^{-3}
2	-1.63×10^{-3}	59.0×10^{-3}

^a Computed error, $E = \hat{S}/S - 1$, versus number of frozen elements (N) for conventional (c) and Galerkin (G), flux calculations. There are $3N$ liquid elements. The thermal parameters for the frozen (liquid) domains are $c = 0.62(0.70)$ cal/°C/cm³; $K = 0.0096(.0069)$ cal/cm/sec/°C; $L = 17.68$ cal/cm³; $\Delta T = 10.0(4.0)$ °C; $\lambda = 0.35055$. The temporal resolution $M = 64$.

POLAR ANALYSIS AND TESTS

In cylindrical coordinates we have the 1-D heat equation

$$Rc \frac{\partial T}{\partial t} - \frac{\partial}{\partial R} \left(RK \frac{\partial T}{\partial R} \right) = 0 \quad (25)$$

and an analytic solution for a line heat sink Q at the origin [5]. For a one-phase problem with N linear elements, the Galerkin equation for the heat flux at S is

$$L(SV_N)^G = \left\langle Rc \frac{\partial \hat{T}}{\partial t}, \phi_N \right\rangle + \frac{\bar{R}}{S} \left(SK \frac{\partial \hat{T}}{\partial R} \Big|_N \right), \quad (26)$$

where \bar{R} is the average value of R in the boundary element. The conventional differentiation of \hat{T} gives

$$L(SV_N)^c = SK \frac{\partial \hat{T}}{\partial R} \Big|_N. \quad (27)$$

As in the Cartesian case, the Galerkin equation contains an extra heat storage term. Additionally, however, Eq. (26) differs from (27) by the geometric factor $\bar{R}/S = (1 - (1/2N))$ in the conduction term. For freezing problems, both features contribute to the overprediction of V_N by the conventional approach and both effects are linear in the mesh spacing.

To quantify the error accumulation in $S(t)$, we proceed as in the Cartesian case, assuming a numerical solution $\hat{T} = \hat{T}(\rho)$, where $\rho = R/S(t)$. Evaluation of (26) yields, ignoring the terms in $1/N^2$,

$$L(SV_N)^G = K \frac{d\hat{T}}{d\rho} \Big|_N \left[1 - \frac{1}{2N} - \frac{c}{K} \frac{S}{2N} V_N \right], \quad (28)$$

which may be easily integrated as

$$\left(\frac{S^2}{2} \right)^G = \frac{K}{L} \frac{d\hat{T}}{d\rho} \Big|_N \left[\left(1 - \frac{1}{2N} \right) \left(1 + \frac{c}{2NL} \frac{d\hat{T}}{d\rho} \Big|_N \right)^{-1} \right] t. \quad (29)$$

The conventional version (27) may also be easily integrated,

$$\left(\frac{S^2}{2} \right)^c = \frac{K}{L} \frac{d\hat{T}}{d\rho} \Big|_N t. \quad (30)$$

With the analytic estimate $d\hat{T}/d\rho|_N \simeq 2\lambda^2 L/c$, we find

$$\frac{S^c}{S^G} = \left[\frac{1 + \lambda^2/N}{1 - (1/2N)} \right]^{1/2} \simeq 1 + \frac{\lambda^2}{2N} + \frac{1}{4N}. \quad (31)$$

The first term, $\lambda^2/2N$, is the same as in the Cartesian case, and stems from the heat

storage term in (26). When the latent heat term dominates the heat balance, $\lambda^2 \approx \frac{1}{2}(Qc/2\pi KL)$ and by analogy with the Neumann case we identify $Qc/2\pi KL$ as the Stefan number for this problem. The second term in (31), $1/4N$, is due to the geometric effect in the conduction term. In many practical situations, $\lambda^2 \ll 1$ and this effect will be dominant—in which case the heat imbalance is independent of thermal properties.

We performed numerical experiments similar to those in the Cartesian case, with a mesh of N linear elements initialized as in [6]. The temporal discretization error was second order for both conventional and Galerkin phase flux calculations, as expected. Figure 5 shows the isolated spatial error versus N using conventional flux calculations at the phase boundary. The error is linear in N , as predicted, and of the same magnitude as its Cartesian counterpart for the same Stefan number. The Galerkin flux calculation consistently reduced the total computed error a hundred-fold relative to the conventional method, and is second order in N as shown in Fig. 6. Figure 7 shows the asymptotic error as a function of S for various values of N and compares it to that predicted by (31). The experimental results clearly show excellent agreement with the simple analysis. Similar success was obtained for test cases where $\lambda^2 \ll 1$. In this situation, the second term in (31) is dominant. Conven-

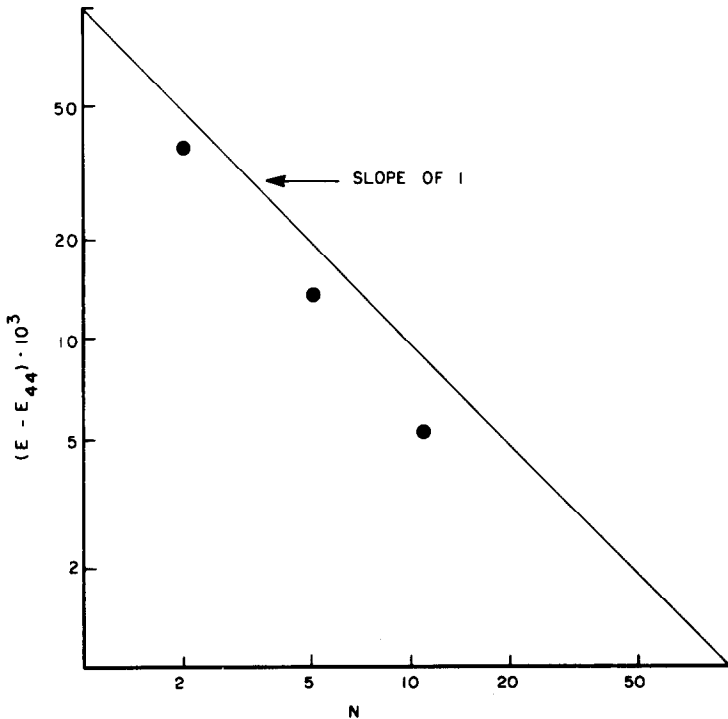


FIG. 5. Isolated spatial error using conventional flux calculation versus N for 1-D, 1-phase polar tests.

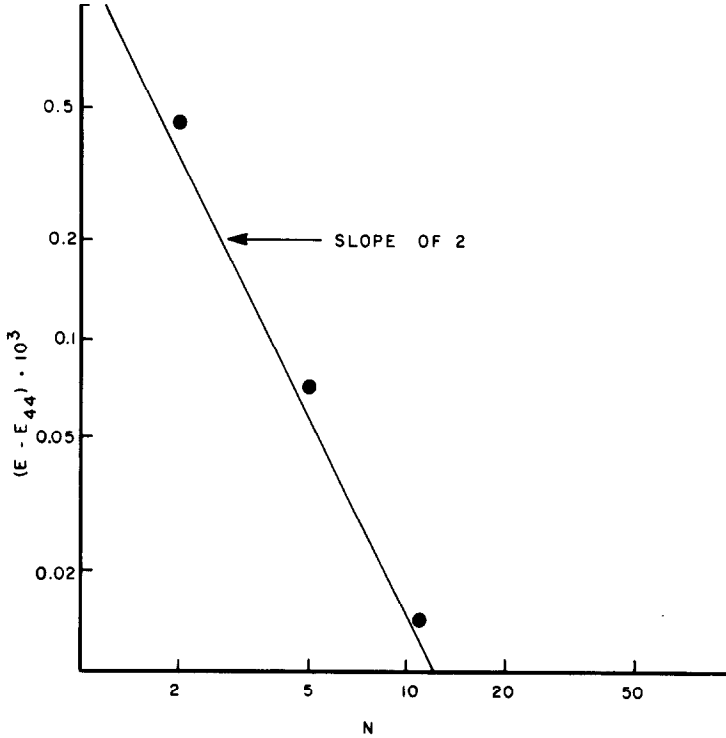


FIG. 6. Isolated spatial error using Galerkin flux calculation versus N for 1-D, 1-phase polar tests.

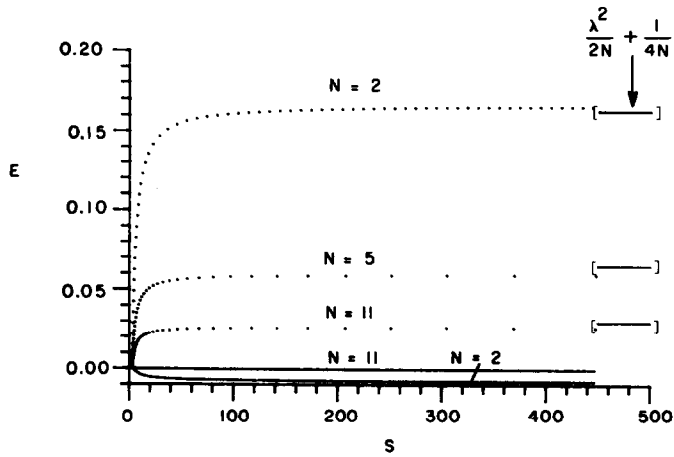


FIG. 7. Asymptotic relative error for various values of N for 1-D, 1-phase polar tests. The conventional flux error (\cdots); the error estimate, Eq. (31) ($[\]$); Galerkin flux error ($-$).

tional phase front errors were essentially independent of thermal properties as expected.

A complementary set of two-phase, 1-D results were obtained in this geometry; they were consistent with all the above discussion and analysis.

Finally, we have solved a set of 1- and 2-phase polar problems on a 2-D grid of linear triangles as in [6]. With reasonable circumferential resolution these results converged to their 1-D counterparts, as expected, and conclusions with respect to the radial resolution are unchanged. In Fig. 8 we isolate the circumferential discretization error for a typical run by subtracting off the error obtained in the limiting 1-D polar simulation. The results for both conventional and Galerkin phase boundary treatment are essentially the same. Evidently, the addition of a second dimension tangential to the phase boundary introduces comparable second-order errors regardless of boundary treatment.

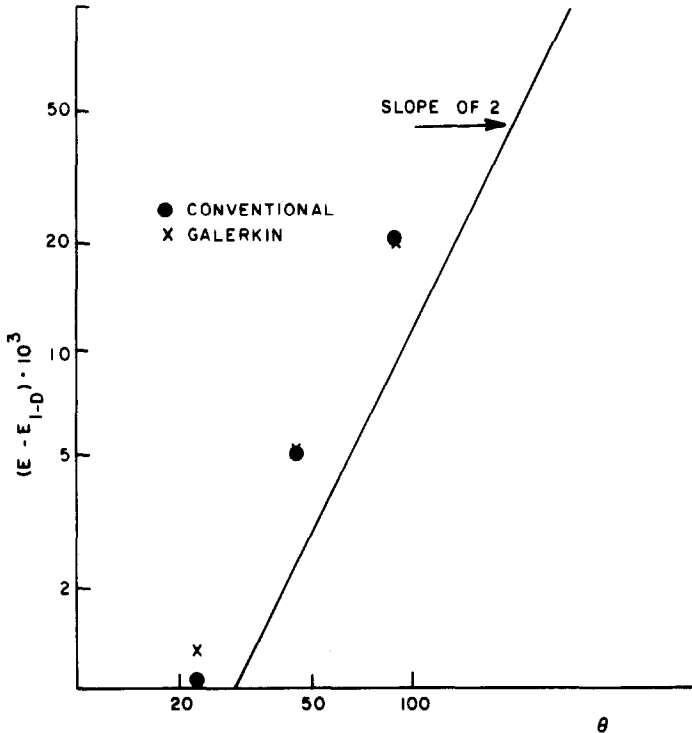


FIG. 8. Circumferential discretization error for conventional and Galerkin flux calculations at the phase boundary. $\Delta\theta = \theta/4$.

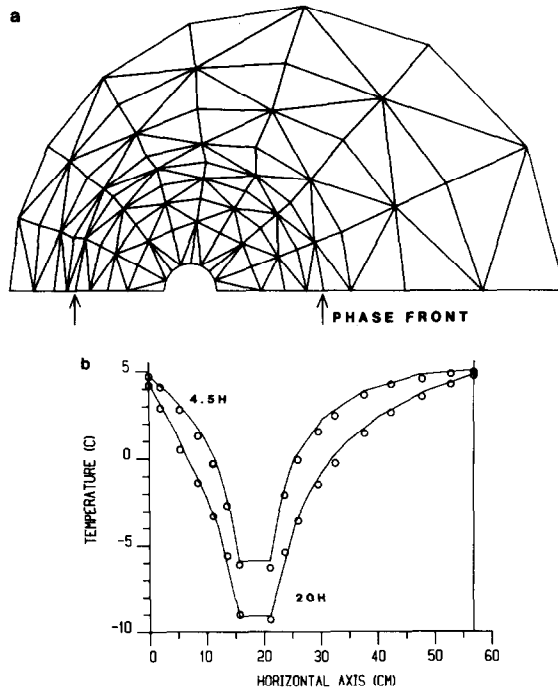


FIG. 9. Computed and lab results for drum experiment [11]. (a) Mesh after 20h, (b) temperature along axis of symmetry after 4.5 and 20h. Numerical results (—); data (○).

COMPARISON WITH LAB DATA

Recently, O'Neill [11] introduced a test case based on laboratory freezing of a saturated coarse sand confined in a cylindrical drum. Freezing was initiated by an eccentrically placed cold pipe; temperature was maintained above freezing on the drum circumference. In Fig 9 we show computed results versus the data, which Dr. O'Neill kindly provided.

SUMMARY AND CONCLUSION

It is shown that a perfect heat balance is maintained in multidimensional deforming element phase change simulation, provided one utilizes the complete set of Galerkin equations. At boundaries where temperature is specified, the associated Galerkin equation is "the equation for the heat flux."

It is, however, conventional practice to discard the Galerkin equations along type I boundaries. Use of this procedure on the phase boundary leads to a heat imbalance which arises in the differentiation of the numerical temperature solution

and which may be quantified for simple problems. Both analysis and experiment indicate that this heat imbalance produces an error which is first-order in the mesh spacing normal to the boundary and which dominates the overall numerical error for realistic sets of parameters. Retention of the Galerkin equation on the phase boundary as the vehicle for calculating the boundary motion restores the second-order accuracy on linear elements.

Operationally, this new procedure is easily implemented. Following assembly of the Galerkin set, we remove *and save* the equations at the phase boundary nodes, compute simultaneously the nodal temperature changes dT_i/dt as usual, and then compute the latent heat balance via the saved equations and the new temperature information. Parallel conclusions have also been established [7, 12] for parabolic problems on fixed domains.

Finally, we note that a similar set of conclusions have been reached by Bonnerot and Jamet [1-4], in the separate context of space-time finite elements. Their early [1, 2] experiments utilized conventional treatment of the phase boundary flux on linear one- and two-dimensional elements, and showed first-order accuracy. In one dimension, second order was achieved by a quadratic reinterpolation of \hat{T} at the phase boundary, but the approach is not readily applicable in higher dimensions. Subsequently, one-dimensional quadratic elements were adopted and conventional differentiation of \hat{T} gave second-order accuracy, while cubic reinterpolation gave third-order results. Bonnerot and Jamet [4] introduced a one-dimensional improvement which, like our own method, has the property $\sum \phi_i = 1$ and which therefore conserves heat; third-order results were obtained on the one-dimensional quadratic elements without recourse to reinterpolation. Given the underlying similarity of their method to ours [6], the present results complement these findings.

ACKNOWLEDGMENT

This work has been supported by the U.S. Army Cold Regions Research and Engineering Laboratory under Contract DACA89-82-K-0004.

REFERENCES

1. R. BONNEROT AND P. JAMET, *Int. J. Numer. Methods Eng.* **8**, (1974), 811.
2. R. BONNEROT AND P. JAMET, *J. Comput. Phys.* **25** (1977), 163.
3. R. BONNEROT AND P. JAMET, *J. Comput. Phys.* **32** (1979), 145.
4. R. BONNEROT AND P. JAMET, *J. Comput. Phys.* **41** (1981), 357.
5. H. S. CARSLAW AND J. C. JAEGER, "Conduction of Heat in Solids," 2nd ed., pp. 295-296, Clarendon, Oxford, 1959.
6. D. R. LYNCH, *J. Comput. Phys.* **47** (1982), 387.
7. D. R. LYNCH, *Advances in Water Resources* **7**, (1984), 67.
8. D. R. LYNCH AND W. G. GRAY, *J. Comput. Phys.* **36** (1980), 135.
9. D. R. LYNCH AND K. O'NEILL, *Int. J. Numer. Methods Eng.* **17** (1981), 81.

10. K. O'NEILL AND D. R. LYNCH, Chap. 11, "Numerical Methods in Heat Transfer" (Lewis *et al.*, Eds.), J. Wiley, New York, 1981.
11. K. O'NEILL, *Int. J. Numer. Methods Eng.* **19** (1983), 1825.
12. P. M. GRESHO, R. L. LEE, R. L. SANI, *in* "Numerical Methods in Thermal Problems," Vol. 2 (R. W. Lewis, K. Morgan, B. Schrefler, Eds.), pp. 663-675, Pineridge, Swansea, 1981.

RECEIVED: August 16, 1983; REVISED March 30, 1984

DANIEL R. LYNCH AND JOHN M. SULLIVAN, JR.

*Thayer School of Engineering,
Dartmouth College,
Hanover, New Hampshire 03755*